PV-PPV: Parameter Variability Aware, Automatically Extracted, Nonlinear Time-Shifted Oscillator Macromodels

Zhichun Wang, Xiaolue Lai and Jaijeet Roychowdhury
Department of Electrical and Computer Engineering, University of Minnesota
Email: {wangzc, laixl, jr}@umn.edu

Abstract— **The PPV is a robust phase domain macromodel for oscillators. It has been proven to predict oscillators' responses correctly under small signal perturbations, and capture nonlinear phase effects such as injection locking/pulling. In this work, we present a novel approach to extend the PPV macromodel to handle variability in circuit parameters. We derive a modified PPV-based phase equation in which parameter variations are modelled as special inputs. An important feature of our technique is that it avoids PPV re-extraction, this resulting in great convenience and efficiency in its use for, *e.g.*, Monte Carlo type simulations. Using LC and ring oscillators as examples, we demonstrate the capability of the proposed technique for capturing parameter variation effects in injection locking analysis. Simulation results show that our new approach accurately predicts the maximum locking range of oscillators with speedups of two orders of magnitude over direct simulation.**

Categories & Subject Descriptors:
B.7.2 [INTEGRATED CIRCUITS]: Design Aids—Simulation, Verification.
J.6 [COMPUTER-AIDED ENGINEERING]: Computer-aided design (CAD).
General Terms: Algorithms, Theory, Verification.
Keywords: PPV, parameter variation, injection locking, nonlinear macromodels, oscillator phase response.

I. Introduction

Oscillators are important circuit components in both analog and digital systems. For example, in communications, oscillators are used to generate signal carriers upon which data signals are modulated. In digital systems, different functional blocks are synchronized by clock signals which are generated by phase-locked loops (PLLs) [1]. In spite of the ubiquity of oscillators in circuits, their design continues to present challenges. The difficulties stem fundamentally from oscillators' innate neutral phase stability, which makes them very sensitive to any kind of interference, including circuit parameter variations [2] and external noise perturbations. Before an oscillator design is finally taped out and sent for fabrication, intensive simulations are typically performed to best ensure that the system works well under worst case scenarios.

Direct time-domain simulation of oscillator-based systems at the level of SPICE [3] is typically impractical because of its great inefficiency. Transient simulation algorithms easily accumulate large numerical errors in phase due to oscillators' neutral phase stability, resulting in inaccurate frequency estimations. To limit simulation inaccuracy, very small timesteps (*e.g.*, many hundreds of steps per cycle) need to be used in oscillator simulations. In some oscillator-based systems (*e.g.*, PLLs with large divide ratios), transients can last hundreds of thousands of cycles. With each cycle requiring hundreds of small timesteps for accurate simulation of the embedded voltage-controlled oscillator (VCO), simulations can last days or even weeks. This efficiency problem is further aggravated when parameter variations need to be considered. Designers need to simulate the same circuit hundreds/thousands times to find the worst case. As a result, devising more efficient and accurate simulation approaches is important.

To improve simulation efficiency for oscillator-based systems, phase macromodelling techniques are widely used. In such approaches, a small phase-domain oscillator macromodel is used to replace the original oscillator circuit. The much smaller phase macromodel has much better numerical efficiency due to its small size; furthermore, operating in the phase domain enables simulations to take much larger timestep than possible in the voltage/current domains of full SPICE-level simulation. To ensure accuracy, however, it is of paramount importance to use a phase macromodel which correctly captures the oscillator's response to perturbations. Whereas various phase-domain oscillator macromodels have been proposed [4]–[7], it has been well established in recent years [8]–[12] that the perturbation projection vector (PPV) macromodel proposed in [7] is the best currently available. The PPV macromodel is not only able to predict the phase responses of oscillators under small signal perturbation accurately, but it also correctly captures nonlinear phase effects (*e.g.*, injection locking, phase pulling) as well as a variety of other effects [8], [9].

The PPV macromodel combines a scalar, nonlinear time-shifted phase equation [7], [13], [14] with a small linear periodic time-varying (LPTV) system for capturing slowly-dying amplitude variations [15]. The nonlinear phase equation captures the phase response of the oscillator under the influence of perturbations, and the LPTV amplitude macromodel can be incorporated in case when second-order effects due to amplitude variations are important and need to be considered. The PPV macromodel has many applications, including predicting injection locking in oscillators [8], and estimating phase jitter and transient response of PLLs under loop nonidealities [9]. However, the PPV macromodel, as developed so far, only predicts oscillator behavior under electrical perturbations (such as power supply interference and thermal noise); it is not variability aware, *i.e.*, it does not take into account, *e.g.*, random and systematic process variations.

Nowadays, chip design is in the deep-submicron era: devices are becoming smaller and smaller, and fabrication techniques cannot guarantee that devices have identical parameters. Parameter variability is playing an increasingly important rôle in limiting chip performance and correctness; indeed, it has become possibly the most crucial issue in circuit design. Simulations using nominal design parameters are no longer sufficient, since achieving them in fabrication is more the exception than the rule. Designers run Monte-Carlo simulations over many combinations of varying parameters, requiring hundreds, thousands or even millions of simulations, to ensure that worst case performances still remain within spec. The obvious way to use PPV macromodels for parameter variability analyses is to simply re-extract the PPV macromodel for each choice of parameters. This is, however, computationally expensive, since it involves a steady-state solution (such as shooting [16] or harmonic balance [17]) of the full SPICE circuit in every Monte-Carlo run. Hence, there has been considerable interest in PPV macromodels that embed circuit parameters directly and do not require re-extraction when parameters change.

In this work, we extend the PPV approach by directly embedding

Permission to make digital or hard copies of all or part of this work for personal or classroom use is granted without fee provided that copies are not made or distributed for profit or commercial advantage and that copies bear this notice and the full citation on the first page. To copy otherwise, or republish, to post on servers or to redistribute to lists, requires prior specific permission and/or a fee.
DAC 2007, June 4–8, 2007, San Diego, California, USA.
Copyright 2007 ACM 978-1-59593-627-1/07/0006 ...$5.00.

varying circuit parameters into the macromodel. We derive a new nonlinear phase equation which not only predicts the phase response due to electrical perturbations applied to the oscillator, but also captures the impact of parameter variability on the oscillator's phase deviations simultaneously. A crucially important feature of our approach is that the oscillator's variability-equipped PPV macromodel *does not need to be re-extracted* when circuit parameters are changed. Instead, it needs to be extracted only once for the nominal circuit; by virtue of its directly incorporating the circuit's varying parameters and avoiding repeated extraction, this PPV macromodel provides large speedups for Monte-Carlo simulations.

We evaluate our technique on LC and ring oscillators, predict the maximum locking range of injection locking, and compare results with SPICE-level full transient simulation and the original PPV macromodel. In each case, circuit parameters are chosen to varying and two situations – when the external perturbations exist and do not exist – are simulated. Numerical results show that the new variability-equipped PPV macromodel is able to correctly predict oscillator phase responses and locking ranges in the presence of parameter variation.

The remainder of the paper is organized as follows. In Section II, we briefly introduce the PPV macromodel. In Section III, we derive an improved nonlinear phase equation that is able to predict the phase response of oscillators due to parameter variations. In Section IV, we validate the new phase equation by predicting injection locking in LC and ring oscillators.

II. Previous Work – PPV Macromodel

In this section, we briefly introduce the PPV macromodel, and discuss its limitations when parameter variations need to be taken into consideration. For simplicity and clarity, we use ODE form of oscillator equations in this paper[1].

A general oscillator under perturbation can be expressed with an ODE equation

$$\dot{x}(t) + f(x(t)) = b(t), \tag{1}$$

where $b(t)$ is a vector of perturbations applied to the free running oscillator, $x(t)$ is the state variables (*e.g.*, node voltage, branch current,*etc.*) and $f(x)$ models the nonlinearity in the oscillator.

According to [7], the solution of the perturbed oscillator can be expressed as

$$x_p(t) = x_s(t+\alpha(t)) + y(t+\alpha(t)), \tag{2}$$

where $x_s(t)$ is the steady-state solution of the unperturbed oscillator. The effect of the perturbations $b(t)$ is divided into two parts: the phase deviation $\alpha(t)$ and the amplitude variation $y(t+\alpha(t))$.

For deriving macromodels which calculate $\alpha(t)$ and $y(t+\alpha(t))$ under small perturbation $b(t)$, (1) needs to be linearized over its steady state solution

$$\begin{aligned} \dot{o}(t) &\approx -\frac{\partial f(x)}{\partial x}\Big|_{x_s(t)} o(t) + b(t) \\ &= -G(t)o(t) + b(t), \end{aligned} \tag{3}$$

where $x_s(t)$ is the steady state orbit of the oscillator, and $o(t)$ is the small deviation from the steady state $x_s(t)$. (3) is a linear periodic time-varying (LPTV) system. Its homogenous part is

$$\dot{o}(t) = -G(t)o(t). \tag{4}$$

According to the Floquet theory [18], (4) has a set of n linear independent solutions

$$z_i(t) = e^{\mu_i t} u_i(t), 1 \le i \le n. \tag{5}$$

In this equation, n is the system size, μ_i is the Floquet exponent, and $u_i(t)$ is the corresponding Floquet eigenvector, which is a T periodic waveform (T is the oscillator period). For an oscillatory LPTV system, there must exist one Floquet exponent which is 0. For convenience, we choose $\mu_1 = 0$, and the corresponding Floquet eigenvector can be proven [7] to be

$$u_1(t) = \dot{x}_s(t). \tag{6}$$

The derivative of the steady state solution is a solution of the homogenous part of the oscillator LPTV system.

The adjoint system of (4) is

$$\dot{o}^T(t) = o^T(t)G(t), \tag{7}$$

whose solutions can be expressed as

$$w_i(t) = e^{-\mu_i t} v_i(t), 1 \le i \le n. \tag{8}$$

$v_i(t)$ is the Floquet eigenvector of the adjoint system. We also have $\mu_1 = 0$, and the corresponding Floquet eigenvector $v_1(t)$ is a very important quantity, which represents the oscillator's phase sensitivity to perturbations. $v_1(t)$ is called "perturbation projection vector (PPV)" in [7]. $u_i(t)$ and $v_i(t)$ satisfy biorthogonality conditions

$$v_i^T(t)u_j(t) = \delta_{ij}. \tag{9}$$

It has been shown in [7] that the oscillator phase deviation $\alpha(t)$ due to the perturbation $b(t)$ is governed by a scalar, nonlinear time-shifted differential equation

$$\dot{\alpha}(t) = v_1^T(t+\alpha(t)) \cdot b(t) \tag{10}$$

The amplitude variations $y(\hat{t})$ is a linear combination of $\{z_2(\hat{t}), ..., z_n(\hat{t})\}$ which satisfies

$$v_1^T(\hat{t}) \cdot y(\hat{t}) = 0, \tag{11}$$

where $\hat{t} = t + \alpha(t)$.

In (10), the PPV is a vector of waveforms with size of n (the oscillator's system size). Each waveform represents the oscillator's phase sensitivity to perturbation injected to the corresponding circuit node. $b(t)$ is a also vector of size n, representing the perturbations applied to each oscillator node. The dot product translate these two vectors into a scalar, as a result, we obtain a simple one-dimensional differential phase equation which has very good numerical stability and is very easy for solving.

The PPV waveforms, which are crucial for solving (10), can be extracted from the SPICE-level description of oscillator circuits by numerical methods effectively [7], [14] both in the time domain and the frequency domain. Once the PPV waveforms are available, (10) can be solved efficiently and the oscillator's phase deviation is obtained. It has been demonstrated that (10) is an exact oscillator phase model for small signal perturbations [7] which captures oscillators' phase deviation accurately when the perturbation is relatively small. And (10) is a nonlinear equation, which is proven to be able to capture nonlinear phase effects (*e.g.*, injection locking) in oscillators [8].

Even though the PPV macromodel has many advantages, it fails when the parameter variation in the circuit needs to be considered. No terms of parameter being explicit in (10), this equation cannot capture phase deviation due to parameter variations. Indeed, PPV waveforms contain the parameters implicitly, therefore they have to be re-extracted if any parameter is changed in the circuit. This limitation greatly slows down the Monte Carlo type simulation.

III. New PPV Equation With Process Variation Consideration

In this section, we derive an improved oscillator phase equation, in which phase deviation due to parameter variation is able to be captured.

We start from the oscillator ODE equation. However, this time we consider circuit parameters, and add the circuit parameter term p to (1)

$$\dot{x}(t) + f(x(t), p) = b(t). \tag{12}$$

In this new equation, the nonlinear $f()$ is not only the function of state variables $x(t)$, but also the function of circuit parameter p.

[1]The theory can be easily extended to DAE form; our implementation in for general DAEs.

Considering the parameter variations, we have

$$p = p^* + \Delta p, \tag{13}$$

where p^* is the nominal parameter and Δp is the parameter deviations over p^*. Hence, (12) can be rewritten as

$$\dot{x}(t) + f(x(t), p^* + \Delta p) = b(t). \tag{14}$$

Now we assume the steady state solution of the circuit under nominal parameter p^* is $x_s(t)$, or $x_s(t)$ satisfies

$$\dot{x}_s(t) + f(x_s(t), p^*) = 0. \tag{15}$$

The perturbed solution (due to both input $b(t)$ and parameter variation Δp) can be expressed as

$$\begin{aligned} x_p(t) &= x_s(t+\alpha(t)) + y(t+\alpha(t)) && (16)\\ &= x_s(\hat{t}) + y(\hat{t}). && (17)\end{aligned}$$

where $\hat{t} = t + \alpha(t)$. Substituting (17) into (14), we have

$$\frac{d}{dt}(x_s(\hat{t}) + y(\hat{t})) + f(x_s(\hat{t}) + y(\hat{t}), p^* + \Delta p) = b(t) \tag{18}$$

Applying Taylor expansion to (18) over steady state $x_s(\hat{t})$, and dropping all high order terms, we obtain

$$\dot{x}_s(\hat{t})\dot{\alpha}(t) + \dot{y}(\hat{t}) + G(\hat{t})y(\hat{t}) + SF_p(\hat{t})\Delta p = b(t), \tag{19}$$

where $\dot{\alpha}(t) = \frac{d}{dt}\alpha(t)$, $\dot{x}_s(\hat{t}) = \frac{d}{d\hat{t}}x_s(\hat{t})$, $\dot{y}(\hat{t}) = \frac{d}{d\hat{t}}y(\hat{t})$ and

$$\begin{aligned} G(\hat{t}) &= \frac{\partial f}{\partial x}|_{x_s(\hat{t}),p^*} && (20)\\ SF_p(\hat{t}) &= \frac{\partial f}{\partial p}|_{x_s(\hat{t}),p^*} && (21)\end{aligned}$$

There are both phase deviation term $\alpha(t)$ and amplitude variation term $y(\hat{t})$ in (19). To obtain a phase equation like (10), we need a way to cancel out $y(\hat{t})$ term in (19). Considering the relationship of $v_1(\hat{t})$ and $y(\hat{t})$ in (11), we multiply $v_1(\hat{t})$ to both side of (19), and obtain

$$v_1^T(\hat{t})\dot{x}_s(\hat{t})\dot{\alpha}(t) + v_1^T(\hat{t})\dot{y}(\hat{t}) + v_1^T(\hat{t})G(\hat{t})y(\hat{t}) + v_1^T(\hat{t})SF_p(\hat{t})\Delta p = v_1^T(\hat{t})b(t). \tag{22}$$

From (6), we know $u_1(\hat{t}) = \dot{x}_s(\hat{t})$, and $v_1^T(\hat{t}) \cdot u_1(\hat{t}) = 1$ due to biorthogonality between $u_i(t)$ and $v_i(t)$. Hence, we have

$$v_1^T(\hat{t})\dot{x}_s(\hat{t}) = 1. \tag{23}$$

We know $v_1(t)$ is a solution of the adjoint system

$$\dot{o}^T(t) = o^T(t)G(t). \tag{24}$$

Hence, we have

$$\dot{v}_1^T(\hat{t}) = v_1^T(\hat{t})G(\hat{t}). \tag{25}$$

Right multiple $y(\hat{t})$ to both sides of (25) and add $v_1^T(\hat{t})\dot{y}(\hat{t})$ to both side, we get

$$\begin{aligned} v_1^T(\hat{t})\dot{y}(\hat{t}) + \dot{v}_1^T(\hat{t})y(\hat{t}) &= v_1^T(\hat{t})\dot{y}(\hat{t}) + v_1^T(\hat{t})G(\hat{t})y(\hat{t}) && (26)\\ &\Downarrow && (27)\\ v_1^T(\hat{t})\dot{y}(\hat{t}) + v_1^T(\hat{t})G(\hat{t})y(\hat{t}) &= \frac{d}{d\hat{t}}(v_1^T(\hat{t})y(\hat{t})). && (28)\end{aligned}$$

Since $y(\hat{t})$ is amplitude variation, which satisfies (11), we have

$$v_1^T(\hat{t})\dot{y}(\hat{t}) + v_1^T(\hat{t})G(\hat{t})y(\hat{t}) = 0. \tag{29}$$

Considering (22) with (23) and (29), we get

$$\dot{\alpha}(t) + v_1^T(\hat{t})SF_p(\hat{t})\Delta p = v_1^T(\hat{t})b(t). \tag{30}$$

Then we substitute $\hat{t}$ with $t + \alpha(t)$ in (30), and obtain a new phase equation

$$\dot{\alpha}(t) = v_1^T(t+\alpha(t)) \cdot (b(t) - SF_p(t+\alpha(t))\Delta p). \tag{31}$$

Compared to the original PPV phase equation (10), the new phase equation has an extra term $SF_p(t+\alpha(t))\Delta p$, which captures the phase deviation due to parameter variation. Using this new phase equation, we don't need to re-extract the PPV when circuit parameters change. This provides huge speedup. Moreover, the derivation bears the fact that multiple parameter variance can be handled at one time.

IV. Numerical Simulation Results

In this section, we apply the method proposed in Section III to two kinds of oscillators, LC and ring. For both, we extract the PPV on nominal parameters, and then simulate the phase deviation in two cases–with and without external perturbation, while varying some parameters. Results are validated using full circuit transient and harmonic balance simulation. We demonstrate that our new phase equation is able to correctly predict the oscillator's response in the presence of circuit parameter variations and external perturbations, while the original PPV macromodel [7] fails. The results have good match to the full SPICE-level simulation results, with speedups of $30-100\times$.

A. 1-GHz LC Oscillator

Figure 1 shows the block diagram of a negative resistance LC oscillator. Its differential equations are

$$\begin{aligned} \frac{d}{dt}i_L(t) &= \frac{v_C(t)}{L_0} \\ \frac{d}{dt}v_C(t) &= -\frac{i_L(t)}{C_0} - \frac{v_C(t)}{R_0C_0} - \frac{S}{C_0}\tanh\left(\frac{G_n}{S}v_C(t)\right), && (32)\end{aligned}$$

in which R_0, L_0, and C_0 are the resistance, inductance, and capacitance of the LCR tank ($R_0 = 100\Omega, L_0 = 4.869e-7/(2\pi)H, C_0 = 2e-12/(2\pi)F$). S and G_n are parameters of the non-linear negative resistor. These parameters make the circuit oscillate at a resonance frequency of about 1GHz, and the amplitude of the capacitance response voltage v_C is about 0.5852V.

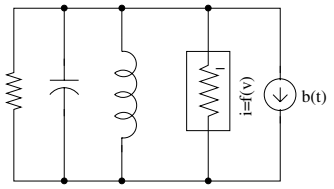

Fig. 1. A simple LC oscillator.

1) Frequency/Phase Deviation Due to Parameter Variations: In this section, we investigate the phase deviation of the oscillator due to circuit parameter variation using our new phase equation, and compare the results with harmonic balance simulation. The inductance is chosen to be the varying parameter.

When there is a $\Delta L/L_0 = 0.005$ variation, the response phase deviation is shown in Figure 2. According to [8], the slope of $\alpha(t)$ stands for the relative frequency difference $\Delta f/f_0$. The result can be validated by a rough hand calculation. The frequency of the simple LC oscillator is $\frac{1}{2\pi\sqrt{(L_0+\Delta L)C_0}}$. Considering $\Delta L/L_0$ is small, we do Taylor expansion to it and drop the high order terms. The frequency can be written as $\frac{1}{2\pi\sqrt{L_0C_0}}(1-\frac{\Delta L}{2\Delta L_0})$. Thus, in the presence of a 0.005 relative variation of the inductance L, the response relative frequency difference $\Delta f/f_0$ will be approximately -0.0025, which is close to our result.

For a precise validation, harmonic balance analysis is performed on several variation points. Figure 3 depicts the relative frequency difference at different variation points, using both the proposed macromodel and harmonic balance analysis. The curves match well when $\Delta L/L_0$ is under 0.02. When the $\Delta L/L_0$ becomes larger, the proposed nonlinear macromodel will lose accuracy, because our new equation is based on the assumption that parameter variation is small.

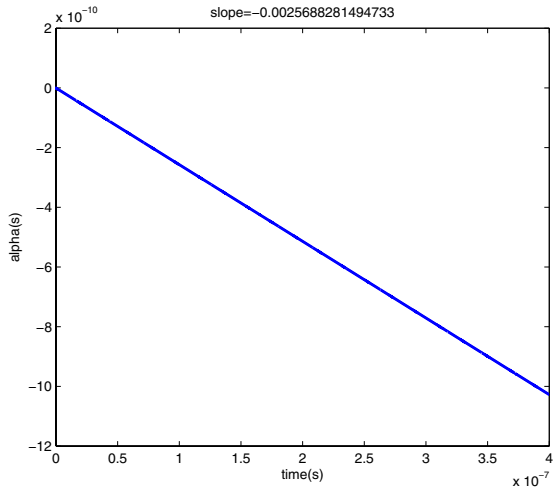

Fig. 2. Phase deviation when L=1.005L_0(LC OSC)

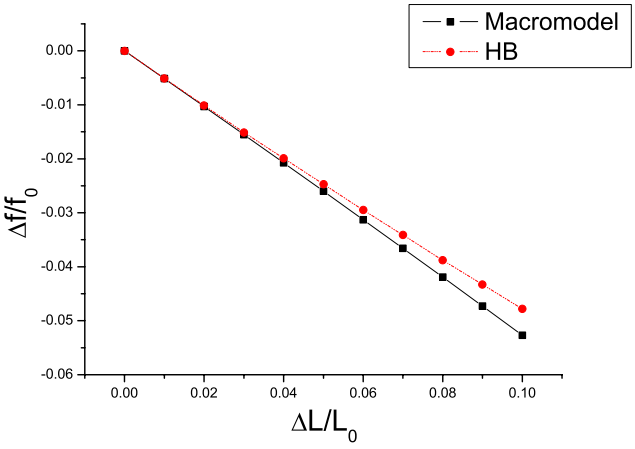

Fig. 3. Frequency Difference VS Parameter Variation(LC OSC)

2) Injection Locking Analysis: In this section, our new equation (31) is used to capture injection locking of the LC oscillator. The inductance is chosen as the varying parameter and the external perturbation is added as a voltage source in series with the inductor. Several simulations are done with different injection magnitude, injection frequency and parameter variation, using both the new equation and full SPICE-like simulation.

In Figure 4, we compare the frequency spectrum of the response between these two methods. $\Delta L/L_0$ is 0.005 and the injection frequency is $1.01f_0$ (f_0 is the natural frequency of the oscillator computed by harmonic balance method). Three injection magnitude case $(0.012, 0.013, 0.014V)$ are simulated. The figures on the left-hand side are from full simulation and those on the right-hand side are from the macromodel. By comparing the spectrum on both side, we find that the result of our proposed macromodel has a good match to that of the full SPICE-like simulation. Vertically the three figures describe the process of injection locking. When the oscillator is not locked to the injection frequency (Figure 4(a)), the response signal has no magnitude at the injection frequency. When the oscillator starts locking to the injection frequency (Figure 4(c)), the response signal has magnitude at both the injection frequency and the original frequency. After the oscillator is locked (Figure 4(e)), fundamental frequency of the oscillator will move to the injection one. Figure 5 plots the time domain response with the injection signal. The magnitudes are normalized for a better display.

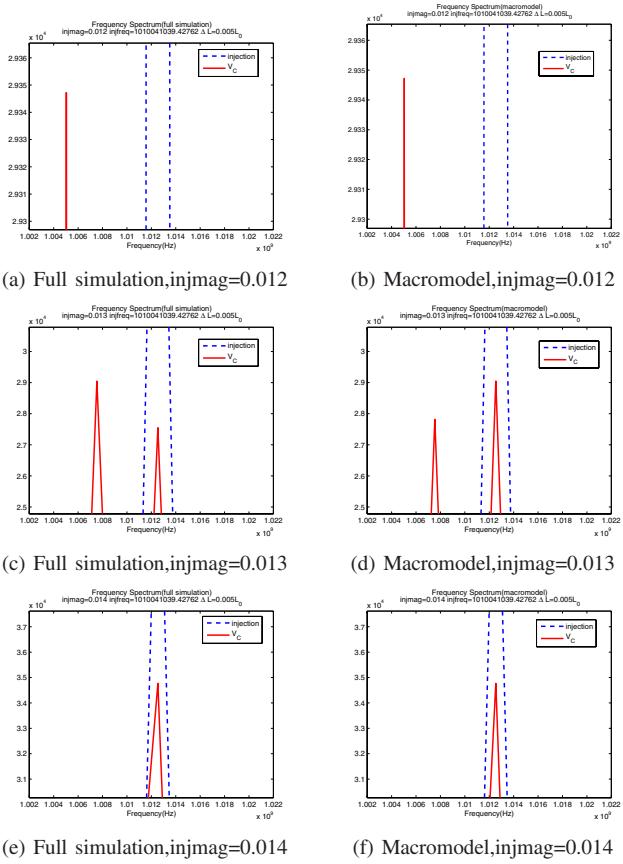

(a) Full simulation,injmag=0.012 (b) Macromodel,injmag=0.012

(c) Full simulation,injmag=0.013 (d) Macromodel,injmag=0.013

(e) Full simulation,injmag=0.014 (f) Macromodel,injmag=0.014

Fig. 4. Procedure of Injection Locking(LC OSC)

By solving (31) at different external perturbations, the locking range, within which the frequency of the oscillator can lock to the injection one, can be determined. Figure 6 plots the locking range calculated by the original macromodel, the new proposed one and the full SPICE-like simulation, when $\Delta L/L_0 = 0.005$. Dash line is the result of the original macromodel, solid line is that of the new proposed one and the "+" is got from full SPICE-like simulation. It is evident that result of our new equation fits that of the full simulation well while the original macromodel fails. Using the macromodel, we obtain speedup of 30×, compared to full SPICE-level simulation.

By calculating the locking range with different parameter variation, we can plot Figure 7, which describes locking range shift induced by parameter variation. We observe that the locking range decreases with the increase of the inductance. This trend is correct because the increase of the inductance causes the natural frequency to drop, hence makes it harder for the oscillator to lock to a perturbation whose frequency is bigger than the natural one. With our proposed technique, capturing this shift requires a low computational cost.

B. Three-Stage Ring Oscillator

Figure 8 shows the block diagram of a three-stage ring oscillator. Its differential equations are

$$\begin{aligned}
\frac{d}{dt}v_1(t) + \frac{v_1}{R_1C_1} - \frac{\tanh(G_{m3}v_3(t))}{R_1C_1} &= 0 \\
\frac{d}{dt}v_2(t) + \frac{v_2}{R_2C_2} - \frac{\tanh(G_{m1}v_1(t))}{R_2C_2} &= 0 \\
\frac{d}{dt}v_3(t) + \frac{v_3}{R_3C_3} - \frac{\tanh(G_{m2}v_2(t))}{R_3C_3} &= 0
\end{aligned} \tag{33}$$

Each stage of this ring oscillator is identical. We have $C_1 = C_2 = C_3 = 2nF$, $R_1 = R_2 = R_3 = 1k\Omega$, and $G_{m1} = G_{m2} = G_{m3} = -5$. The

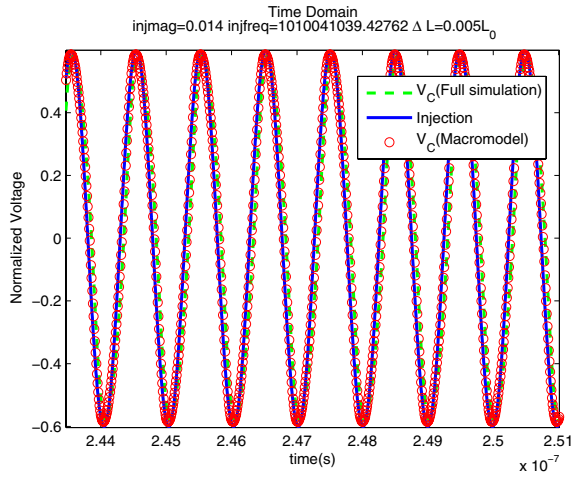

Fig. 5. Time Domain Response under injection locking(LC OSC)

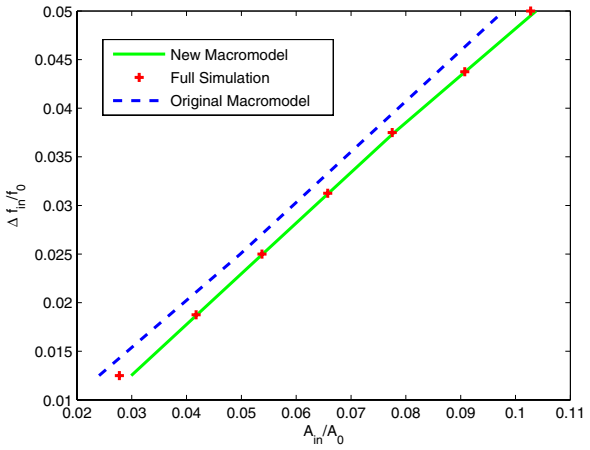

Fig. 6. New locking range validated by full simulation, $\Delta L = 0.005L_0$(LC OSC)

oscillator has a natural frequency of 153498Hz and a maximum load current of $A_0 = 1.2$mA.

1) Frequency/Phase Deviation Due to Parameter Variations: Like the LC Oscillator case, we simulate the phase deviation due to parameter variation. The capacitance in the first stage is chosen to be the varying parameter. We observe that the slope of the phase deviation is -0.058 induced by a 20% relative parameter variation ($\Delta C_1/C_0 = 0.2$), shown in Figure 9.

For this case, the harmonic balance method is also used to validate the results. Figure 10 compares the response relative frequency difference at different variation points. The curves fit well when the $\Delta C1/C_0$ is less than 0.2.

2) Injection Locking Analysis: In this section, (31) is used to capture injection locking of the three-stage ring oscillator. The capacitance is chosen as the varying parameter and the external perturbation is added as a current source at the input node of the first inverter.

Figure 11 plots the locking range calculated by the original macromodel, the new proposed one, and the full SPICE-like simulation, when $\Delta C_1/C_0 = 0.02$. Dash line is the result of the original macromodel, solid line is that of the proposed one and the "+" is from full SPICE-like simulation. This figure also depicts the clear difference between the result of the two macromodels. The result of the our new equation is validated again by the full SPICE-like simulation,

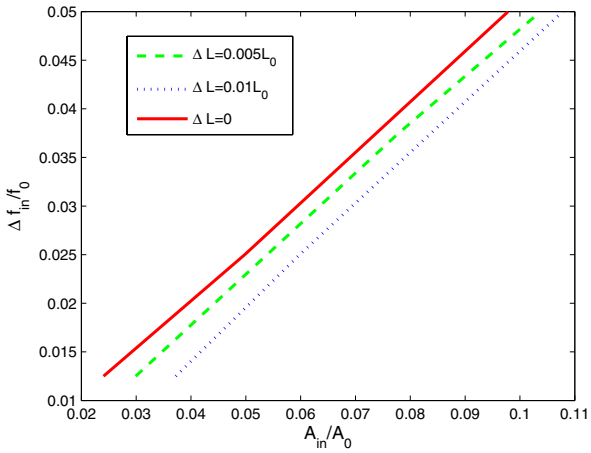

Fig. 7. Locking range shift due to parameter variation(LC OSC)

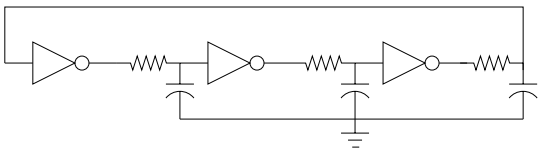

Fig. 8. A three-stage ring oscillator.

shown in Figure 11. Compared to full SPICE-like simulation, we obtain about 100× speedup from the macromodel.

Figure 12 depicts the locking range shift induced by parameter variation. The locking range decreases with the increase of the capacitance. This trend is correct because the increase of the capacitance causes the natural frequency to drop, hence makes it harder for the oscillator to lock to a perturbation whose frequency is bigger than the natural one.

V. Conclusions

We have enhanced the PPV macromodel by equipping it with a direct dependence on varying parameters. The new PPV macromodel remains in the same functional for as originally, except that new "input" are added for parameter variations. We have validated that the PV-PPV macromodel is able to accurately predict oscillator phase responses and injection locking phenomena in the presence

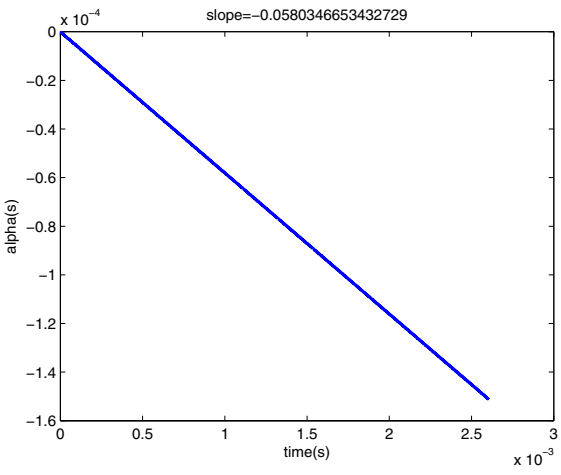

Fig. 9. Phase deviation when C_1=1.2C_0(Ring OSC)

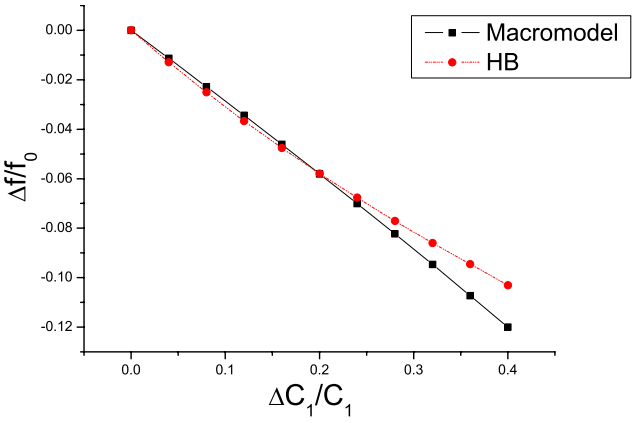

Fig. 10. Frequency Difference VS Parameter Variation(Ring OSC)

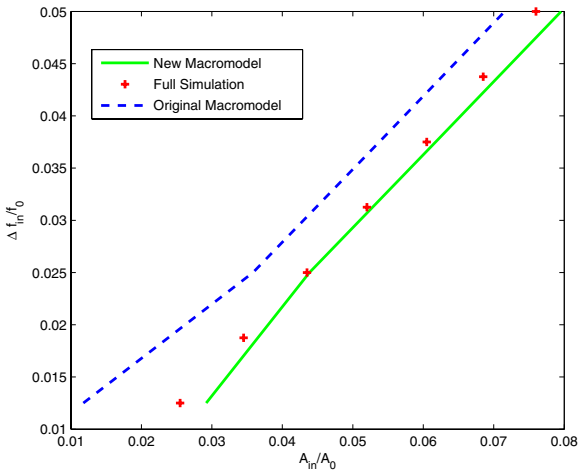

Fig. 11. New locking range validated by full simulation, $\Delta C = 0.02C_0$(Ring OSC)

of significant parameter variations. A crucial feature of PV-PPV is that it removes the need to re-extract oscillator PPV macromodels for every instance of a Monte-Carlo run involving varying circuit parameters.

Acknowledgments

This work has been supported by the Semiconductor Research Corporation, MARCO/GSRC and the National Science Foundation. Computational and infrastructural resources from the Digital Technology Center and the Supercomputing Institute of the University of Minnesota are gratefully acknowledged.

REFERENCES

[1] J.L. Stensby. *Phase-locked loops: Theory and applications*. CRC Press, New York, 1997.

[2] M. Rahman A.A. Mutlu. Statistical methods for the estimation of process variation effects on circuit operations. *IEEE Transactions on Electronics Packaging Manufacturing*, 28:364 – 375, October 2005.

[3] L. Nagel. *SPICE2: A Computer Program to Simulate Semiconductor Circuits*. Electron. Res. Lab., Univ. Calif., Berkeley, 1975.

[4] P. Vanassche, G.G.E. Gielen, and W. Sansen. Behavioral modeling of coupled harmonic oscillators. *IEEE Trans. on Computer-Aided Design of Integrated Circuits and Systems*, 22(8):1017–1026, August 2003.

[5] A. Demir, E. Liu, A.L. Sangiovanni-Vincentelli, and I. Vassiliou. Behavioral simulation techniques for phase/delay-locked systems. In *Proceedings of the Custom Integrated Circuits Conference 1994*, pages 453–456, May 1994.

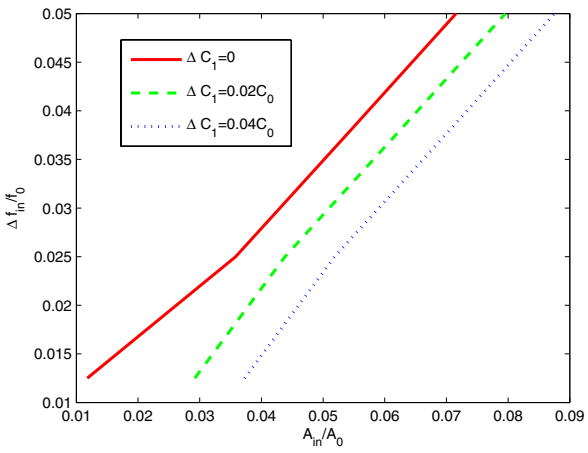

Fig. 12. Locking range shift due to parameter variation(Ring OSC)

[6] A. Hajimiri and T.H. Lee. A general theory of phase noise in electrical oscillators. *IEEE Journal of Solid-State Circuits*, 33(2), February 1998.

[7] A. Demir, A. Mehrotra, and J. Roychowdhury. Phase noise in oscillators: a unifying theory and numerical methods for characterization. *IEEE Trans. on Circuits and Systems-I:Fundamental Theory and Applications*, 47(5):655–674, May 2000.

[8] X. Lai and J. Roychowdhury. Capturing Oscillator Injection Locking via Nonlinear Phase-Domain Macromodels. *IEEE Trans. Microwave Theory Tech.*, 52(9):2251–2261, September 2004.

[9] X. Lai, Y. Wan, and J. Roychowdhury. Fast pll simulation using nonlinear vco macromodels for accurate prediction of jitter and cycle-slipping due to loop non-idealities and supply noise. In *Proc. IEEE Asia South-Pacific Design Automation Conference,*, January 2005.

[10] Y. Wan X. Lai and J. Roychowdhury. Understanding Injection Locking in Negative Resistance LC Oscillators Intuitively Using Nonlinear Feedback Analysis. *Proc. IEEE Custom Integrated Circuits Conference*, 18(21):729 – 732, September 2005.

[11] X. Lai and J. Roychowdhury. Analytical Equations For Predicting Injection Locking in LC and Ring Oscillators. *Proc. IEEE Custom Integrated Circuits Conference*, 18(21):461 – 464, September 2005.

[12] X. Lai and J. Roychowdhury. TP-PPV: Piecewise Nonlinear, Time-Shifted Oscillator Macromodel Extraction for Fast, Accurate PLL Simulation. *Proc. IEEE International Conference on Computer-Aided Design*, pages 269 – 274, November 2006.

[13] A. Demir, D. Long, and J. Roychowdhury. Computing phase noise eigenfunctions directly from steady-state jacobian matrices. In *IEEE/ACM International Conference on Computer Aided Design*, pages 283–288, November 2000.

[14] A. Demir and J. Roychowdhury. A reliable and efficient procedure for oscillator ppv computation, with phase noise macromodelling applications. *IEEE Trans. on Computer-Aided Design of Integrated Circuits and Systems*, 22(2):188–197, February 2003.

[15] X. Lai and J. Roychowdhury. Macromodelling Oscillators Using Krylov-Subspace Methods. *Proc. IEEE Asia South-Pacific Design Automation Conference*, 24(27):6 pp, January 2006.

[16] T. Trick T. Aprille. A computer algorithm to determine the steady-state response of nonlinear oscillators. *Circuits and Systems, IEEE Transactions on [legacy, pre - 1988]*, 19(4):354 – 360, July 1972.

[17] J. White R. Telichevesky, K. Kundert. Efficient AC and noise analysis of two-tone RF circuits. *Proc. IEEE Design Automation Conference*, 3(7):292 – 297, June 1996.

[18] R. Grimshaw. *Nonlinear Ordinary Differential Equations*. Blackwell Scientific, New York, 1990.